

ORIGINAL ARTICLE

S. Benini · W. R. Rypniewski · K. S. Wilson
S. Ciurli · S. Mangani

The complex of *Bacillus pasteurii* urease with β -mercaptoethanol from X-ray data at 1.65-Å resolution

Received: 31 December 1997 / Accepted: 25 February 1998

Abstract The structure of β -mercaptoethanol-inhibited urease from *Bacillus pasteurii*, a highly ureolytic soil micro-organism, was solved at 1.65 Å using synchrotron X-ray cryogenic diffraction data. The structure clearly shows the unexpected binding mode of β -mercaptoethanol, which bridges the two nickel ions in the active site through the sulfur atom and chelates one Ni through the OH functionality. Another molecule of inhibitor forms a mixed disulfide with a Cys residue, thus sealing the entrance to the active site cavity by steric hindrance. The possible implications of the results on structure-based molecular design of new urease inhibitors are discussed.

Key words Urease · *Bacillus pasteurii* · X-ray · Nickel · β -Mercaptoethanol

Introduction

The enzymatic hydrolysis of urea by the Ni-containing enzyme urease (urea amidohydrolase E.C. 3.5.1.5) occurs at a rate 10^{14} times faster than the rate of the uncatalysed reaction, eventually yielding ammonia and carbon dioxide [1–4]. The reaction causes an abrupt increase of pH because of the balanced hydrolysis of the

reaction products. This pH increase is the major cause of the negative side effects of the action of urease in both medical and agricultural applications. Urease serves as a virulence factor in human and animal infections of the urinary and gastrointestinal tracts [2, 4, 5], while high urease activity during soil nitrogen fertilisation with urea (the most used fertiliser world-wide) causes loss of ammonia by volatilisation, inducing plant damage by ammonia toxicity and soil pH increase [2, 6, 7]. Therefore, control of the rate of urea hydrolysis through urease inhibitors would lead both to enhanced efficiency of urea nitrogen uptake by plants and to improved therapeutic strategies for treatment of infections by ureolytic bacteria. Di-phenols, quinones, hydroxamic acids, phosphoramides and thiols have been tested as urease inhibitors in both medicine [2, 4, 8] and agriculture [2, 7, 9, 10]. However, the efficiency of the presently available inhibitors is low, and they cause negative side effects both to humans [2, 4, 11, 12] and to the environment [2, 13]. The discovery of new and more efficient inhibitors has so far relied upon extended screen tests [14]. The present report provides new and detailed structural information on both the binuclear Ni centre in the enzyme active site and the mode of thiol inhibition, vital for structure-based rational design of urease-related drugs.

The report of the X-ray structure of native urease from *Klebsiella aerogenes* at 2.2-Å resolution (R factor=17.3%) (PDB code: 1FWJ) [15, 16], together with the structure of the apoenzyme and several mutants [16–19], provided the first 3-D structural model of the enzyme. In native *K. aerogenes* urease, the two Ni(II) ions in the active site are held at a distance of 3.6 Å by the single bridging carboxylate group of a carbamylated Lys residue. Both Ni(1) and Ni(2) ions are further coordinated by two His residues, while Ni(2) is also bound to an Asp residue. In the most recent model, the additional electron density found in the neighbourhood of the Ni ions, and indeed bridging them, has been interpreted as water molecules, making Ni(1) penta-coordinated and Ni(2) hexa-coordinated in pseudo-octahe-

S. Benini · W. R. Rypniewski
European Molecular Biology Laboratory, c/o DESY,
Notkestrasse 85, D-22603 Hamburg, Germany

K. S. Wilson
Department of Chemistry, University of York, Heslington,
York, YO1 5DD, United Kingdom

S. Ciurli (✉)
Institute of Agricultural Chemistry, University of Bologna,
Viale Berti Pichat 10, I-40127 Bologna, Italy
Fax: +39-51-243362; e-mail: scieurli@agrsci.unibo.it

S. Mangani (✉)
Department of Chemistry, University of Siena, Pian dei
Mantellini, 44 I-531000 Siena, Italy
Fax: +39-577-280405; e-mail: mangani@unisi.it

dral environments [19]. The structure of a *K. aerogenes* C319A mutant urease complexed with the competitive inhibitor acetohydroxamic acid (AHA) (2.0-Å resolution, 92% completeness, R factor=20.4%) has also been reported [19]. In the proposed model, the hydroxamate oxygen asymmetrically bridges the two Ni ions [Ni(1)–O=2.6 Å; Ni(2)–O=1.8 Å], while the carbonyl oxygen of AHA is further bound to Ni(1) at 2.0 Å, in a chelate mode. The Ni–Ni distance is 3.7 Å, suggesting that this separation does not vary substantially upon inhibitor binding. The coordination mode of AHA to the active site of *K. aerogenes* urease is analogous to the structure of a synthetic model compound [20].

The highly conserved amino acid sequences of all known ureases [4,17] and the constant presence of two Ni ions and of their ligands in the active sites [3] imply a common catalytic pathway. Therefore, detailed structures of ureases isolated from different sources will allow a comparison of their molecular features, essential in establishing common properties useful in designing inhibitors effective on a broad range of microbial ureases. The primary structure of the three subunits constituting *K. aerogenes* urease [21] is homologous [identity 63% (α), 46% (β) and 61% (γ), respectively] with that of urease isolated from the alkaliphilic and highly ureolytic soil bacterium *Bacillus pasteurii* [22–24], and the amino acid residues ligating the two Ni ions in the active site are conserved [25]. Ni-edge X-ray absorption spectroscopy data of native *B. pasteurii* urease indicated that the average coordination environment of the two Ni ions is represented by five or six N/O ligands arranged in a pseudo-octahedral geometry, with two of the ligands being histidine imidazole side chains [26]. The crystallisation and cryogenic synchrotron X-ray data collection of *B. pasteurii* urease inhibited with β -mercaptoethanol (β -ME), known to act as a competitive inhibitor of urease [27], have been recently reported together with the description of the structure solution by molecular replacement using the native *K. aerogenes* urease as search model [28]. We describe here the structure of β -ME-inhibited urease from *B. pasteurii* refined at high resolution (1.65 Å, 98.7% completeness, R factor=15.8%), and discuss the possible implications of its features on the catalytic and inhibition mechanisms.

Materials and methods

Protein isolation and crystallization

B. pasteurii urease was isolated and purified to a specific activity of ca. 2500 units/mg as previously reported [24]. The enzyme is heteropolymeric and consists of three subunits ($M_r(\alpha)$ =61.4 kDa; $M_r(\beta)$ =14.0 kDa; $M_r(\gamma)$ =11.1 kDa [25]). β -ME-inhibited urease was crystallised at 20°C from an 11-mg/mL enzyme solution in 20 mM sodium citrate at pH 6.3 using the hanging drop method as reported [28]. Rice-shaped crystals of about 0.4×0.4×0.7 mm formed in few days when the above solution was equilibrated against a precipitant solution containing 53% of saturated ammonium sulfate solution, 1.2 M LiCl and 4 mM β -ME in the same buffer.

ium sulfate solution, 1.2 M LiCl and 4 mM β -ME in the same buffer.

Data collection and reduction

Diffraction data were collected on a single crystal of the protein using synchrotron radiation at 100 K from the BW7B wiggler line [29] (λ =0.8855 Å) of the DORIS storage ring at the EMBL outstation at the Deutsches Elektronen Synchrotron (DESY) in Hamburg (Germany), using a 30-cm MarResearch imaging plate scanner. The data were processed using the program DENZO and merged with SCALEPACK [30]. The data set used for the structure determination and refinement consisted of 114679 reflections merged from 1172081 measured intensities to 1.65-Å resolution (R-merge=0.076). The data set is 98.7% complete in the 14–1.65 Å range. The highest shell between 1.68 and 1.65 Å is 97.8% complete with R-merge=0.59. The space group was determined to be P6₃22, with unit cell parameters $a=b=131.343$ Å, $c=190.013$ Å. Assuming one $\alpha\beta\gamma$ fragment (86.5 kDa) per asymmetric unit, the volume-to-mass ratio, V_M , is 2.7 Å³/Da, giving a solvent content of 54%. These values are in the normal range found for proteins [31], indicating that four urease $\alpha_3\beta_3\gamma_3$ molecules lie on the special positions of point symmetry 3 present in the cell, as confirmed by the structure solution and refinement.

Structure solution and refinement

The structure was solved by the molecular replacement technique as implemented in the program AMoRe [32], using the structure of *K. aerogenes* urease [15] as a search model. The highest peak in the rotation function gave a correlation coefficient of 12.2%, and the translation search gave the correct solution of the structure with a correlation coefficient of 47.4%. The model obtained after rigid-body refinement of the solution was used to phase reflections. The high quality of the initial electron density maps obtained allowed an almost complete manual rebuilding of the model on the *B. pasteurii* primary sequence [25] using the program O [33]. The model was refined using a sequence of PROLSQ [34, 35] and REFMAC [36] cycles. Ideal geometric parameters were those of Engh and Huber [37]. Water molecules were inserted and refined using the program ARP, keeping only those water molecules having sigma better than 1.3 in the electron density map [38]. No restraints were used in refining the nickel–ligand distances. The structure refined to an R factor ($=\sum|F_o - F_c|/\sum F_o$) of 15.8% for data between 14 and 1.65 Å and rms deviations from ideal distances and ‘angle distances’ of 0.008 and 0.023 Å, respectively. The final model consists of 6056 protein atoms, 2 Ni ions, 2 β -ME molecules and 1013 water molecules. By the PROCHECK criteria the model has 89.7% of the main-chain torsion angles within the ‘allowed regions’ of the Ramachandran plot and 9.2% within the ‘additional allowed regions’. The refined crystallographic coordinates have been deposited in the Brookhaven Data Bank under the accession code 1UBP.

Results and discussion

The structure of *B. pasteurii* urease reveals an $\alpha_3\beta_3\gamma_3$ quaternary structure with three crystallographically related active sites, one in each α subunit. This arrangement is analogous to the *K. aerogenes* enzyme, and the analysis of tertiary and secondary structural elements indicates indeed a high degree of similarity. Only the active site will be described here, while the full description of the structure will be the subject of a subsequent report.

The electron density superimposed onto the refined atomic model of the active site is shown in Fig. 1. The

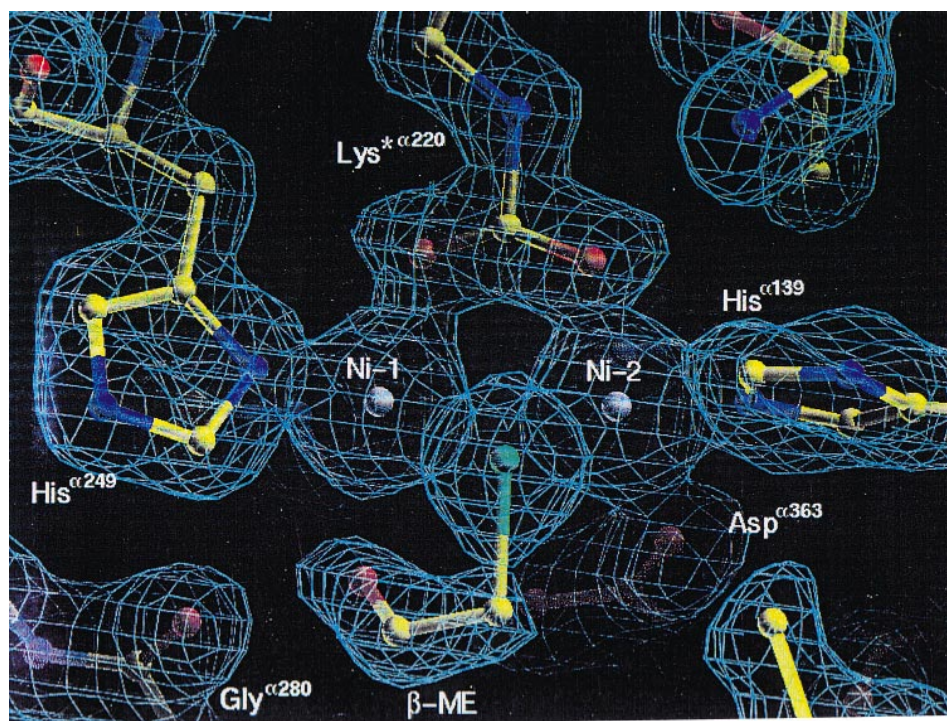


Fig. 1 The atomic model of the active site of β -ME-inhibited *B. pasteurii* urease, showing the Ni coordination environment superimposed on the final $2F_0 - F_c$ electron density map contoured at 1σ

spatial arrangement of the protein ligands to the metal ions in *B. pasteurii* urease complexed with β -ME is similar to that observed in *K. aerogenes* urease both in the native state [16] (PDB code: 1FWJ) and inhibited with AHA [19] (PDB code: 1FWE), resulting in low RMSDs (0.170 Å and 0.173 Å, respectively). Figure 2 shows that two Ni ions are bridged by the carbamylated Lys ^{α 220*} residue. Ni(1) is further bound to His ^{α 249} through the N δ atom and to His ^{α 275} through N ϵ , while Ni(2) is bound to His ^{α 137} and His ^{α 139} through N ϵ , and to Asp ^{α 363} through O δ 1. Both Ni ions are well ordered (B factors of 14.4 and 12.3 Å² for Ni(1) and Ni(2), respectively). The position of conserved amino acid residues not involved in Ni binding but thought to be important in the catalytic mechanism (Ala ^{α 170}, His ^{α 222}, Glu ^{α 223}, Asp ^{α 224}, Gly ^{α 280}, His ^{α 323}, Ala ^{α 366}, Met ^{α 367}) [15, 39], is essentially invariant with respect to the *K. aerogenes* structures, except for His ^{α 323}, proposed to act as the catalytic base in the urea hydrolysis mechanism [39], which shows a large deviation (5 Å) of the imidazole ring atoms farther away from the Ni centre. No density interpreted as water molecules lies within 5 Å from the Ni ions.

The presence of a bridging atom between the two Ni ions, identified as the sulfur of β -ME (final B factor 14.3 Å²), is evident in the electron density map (Fig. 1). The bridging atom was identified in ($3F_0 - 2F_c$) maps when the R factor was ca. 40%, while the whole β -ME molecule was completely evident when the R factor was ca. 30%. The refined model of the inhibitor molecule indicates a chelate binding mode through the terminal OH group, coordinated to Ni(1). The torsional angle of the β -ME molecule is 53°. Charge-transfer transitions observed in the near-UV [40], CD [41], and

MCD [42] spectra of urease in the presence of thiolate competitive inhibitors have been interpreted in the past as indicating direct binding to the Ni(II) ions. Magnetic susceptibility, and variable temperature MCD spectra of β -ME-inhibited urease have shown that the Ni centres are strongly antiferromagnetically exchange-coupled [42, 43], suggesting the presence of a thiolate bridging ligand. This observation was further supported by EXAFS [44, 45]. The present crystallographic study is in agreement with the spectroscopic results, directly revealing the presence of a thiolate ligand bridging the two Ni ions. The only other structurally determined μ -thiolato-bridged cluster in proteins containing Ni ions in the active site is in [Ni,Fe]-hydrogenase, in which the pseudo-tetrahedral Ni ion in the (Cys)₂Ni(Cys)₂Fe cluster core has Ni-S distances of 2.2–2.3 Å and an Ni-S-Fe angle of 67° [46]. The determination of the crystal structure of β -ME-inhibited *B. pasteurii* urease at high resolution further shows the unexpected chelating coordination mode of β -ME to the Ni ions. The ROH-Ni(1) interaction is assisted and stabilised by a strong hydrogen bond donated to the carbonyl oxygen of the conserved Gly ^{α 280} (at 2.4 Å). β -ME is a poor chelating agent because of the low Lewis base character of its OH group, but the hydrogen bond with Gly ^{α 280} enhances the basicity of the hydroxyl oxygen and facilitates binding to Ni(1). These observations provide an enlightening example of how interactions with the protein matrix can modify the chemical behaviour of a molecule, further revealing Gly ^{α 280} as a plausible target for structure-based design of urease inhibitors.

Both Ni ions in the inhibited *B. pasteurii* urease appear to be pentacoordinated (Fig. 3). The coordination geometry around Ni(1) is distorted square-pyramidal,

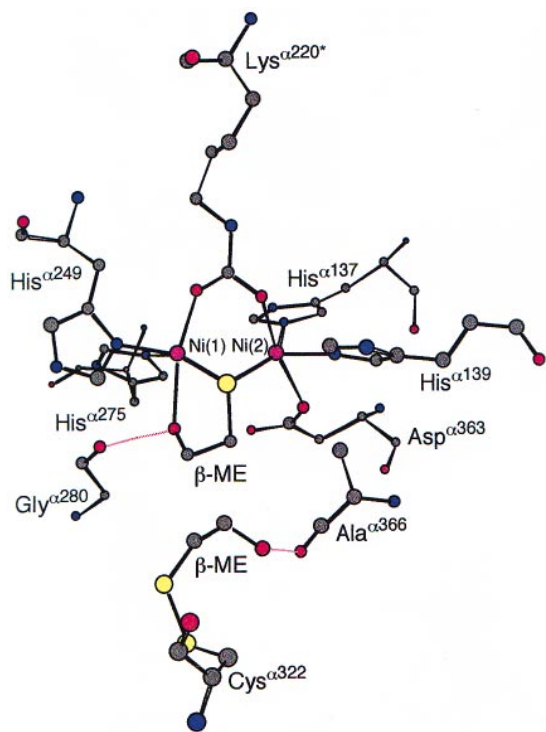


Fig. 2 Refined model of the active-site structure of β -ME-inhibited *B. pasteurii* urease. Hydrogen bonds are shown as red lines.

Key distances: Ni(1)-Lys ^{α 220*} O θ 1 = 2.1 Å; Ni(1)-His ^{α 249} N δ = 2.2 Å; Ni(1)-His ^{α 275} N ϵ = 2.2 Å; Ni(2)-Lys ^{α 220*} O θ 2 = 2.1 Å; Ni(2)-His ^{α 139} N ϵ = 2.1 Å; Ni(2)-His ^{α 137} N ϵ = 2.1 Å; Ni(2)-Asp ^{α 363} O δ 1 = 2.1 Å; Ni(1)-O(β -ME) = 2.3 Å; Ni(1)-S(β -ME) = 2.3 Å; Ni(2)-S(β -ME) = 2.3 Å; Ni(1)-Ni(2) = 3.1 Å.

Key angles: His ^{α 275} N ϵ -Ni(1)-S(β -ME) = 151°; His ^{α 275} N ϵ -Ni(1)-O(β -ME) = 81°; His ^{α 275} N ϵ -Ni(1)-His ^{α 249} N δ = 91°; His ^{α 275} N ϵ -Ni(1)-Lys ^{α 220*} O θ 1 = 100°; O(β -ME)-Ni(1)-S(β -ME) = 75°; S(β -ME)-Ni(1)-Lys ^{α 220*} O θ = 99°; Lys ^{α 220*} O θ 1-Ni(1)-His ^{α 249} N δ = 95°; His ^{α 249} N δ -Ni(1)-O(β -ME) = 100°; His ^{α 249} N δ -Ni(1)-S(β -ME) = 109°; Lys ^{α 220*} O θ 1-Ni(1)-O(β -ME) = 164°; Lys ^{α 220*} O θ 2-Ni(2)-His ^{α 137} N ϵ = 93°; Lys ^{α 220*} O θ 2-Ni(2)-His ^{α 139} N ϵ = 89°; Lys ^{α 220*} O θ 2-Ni(2)-S(β -ME) = 84°; Asp ^{α 363} O δ 1-Ni(2)-His ^{α 137} N ϵ = 84°; Asp ^{α 363} O δ 1-Ni(2)-S(β -ME) = 105°; His ^{α 137} N ϵ -Ni(2)-His ^{α 139} N ϵ = 111°; His ^{α 139} N ϵ -Ni(2)-S(β -ME) = 106°; S(β -ME)-Ni(2)-His ^{α 137} N ϵ = 143°; Lys ^{α 220*} O θ 2-Ni(2)-Asp ^{α 363} O δ 1 = 170°; Ni(1)-S(β -ME)-Ni(2) = 83°

with the equatorial plane constituted by the S and O atoms of β -mercaptoethanol, by the O θ 1 atom of the bridging carbamylated Lys ^{α 220*}, and by the N ϵ of His ^{α 275}, the apical ligand being the N δ of His ^{α 249}. In contrast, the coordination geometry of Ni(2) is best described as distorted trigonal-bipyramidal, with the equatorial plane constituted by the bridging S atom of β -ME and by the N ϵ atoms of His ^{α 137} and His ^{α 139}, the opposite apical ligands being the O θ 2 atom of the bridging carbamylated lysine and Asp ^{α 363} O δ 1. The equatorial planes of the square and trigonal pyramids are joined through the bridging S atom of β -ME, with a dihedral angle between the two average equatorial planes of 63°. The coordination distances between the Ni ions and their protein ligands are, within experimen-

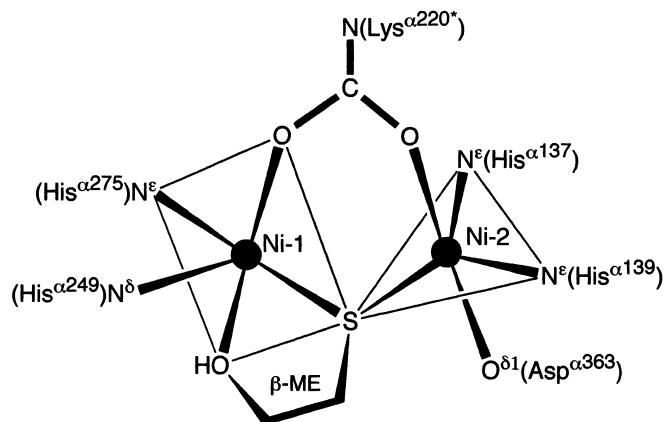


Fig. 3 Schematic idealised representation of the geometry of the Ni centres in β -ME-inhibited *B. pasteurii* urease. Deviations (Å) from least-square plane formed by S(β -ME)-Lys ^{α 220*} O θ 1-His ^{α 275} N ϵ -O(β -ME)-Ni(1) are (respectively): +0.092, +0.053, +0.101, +0.010, -0.257 (RMSD = 0.132 Å); deviations (Å) from least-square plane formed by S(β -ME)-His ^{α 137} N ϵ -His ^{α 139} N ϵ -Ni(2) are (respectively): -0.014, -0.016, -0.010, +0.041 (RMSD = 0.024 Å). The dihedral angle between the two planes is 63°

tal error, the same as those obtained from EXAFS data on native *B. pasteurii* urease (2.03 Å on average) [26]. This observation suggests substantial rigidity of the Ni coordination spheres in this enzyme.

The geometric features of the Ni-S-Ni moiety in β -ME-inhibited *B. pasteurii* urease (Ni-S distances of 2.3 Å; Ni-S-Ni angle of 83°) are consistent with those deduced from EXAFS studies on β -ME-inhibited *K. aerogenes* urease [45] (Ni-S distance of 2.23 Å, Ni-S-Ni angle of 94°), and are similar to those in synthetic model compounds (Ni-S distance of 2.20–2.23 Å, Ni-S-Ni angle of 83.8°–95.2°) [47–50]. The Ni-Ni distance of 3.1 Å, observed in the crystal structure of β -ME-inhibited *B. pasteurii* urease, is similar to the distance of 3.26 Å determined for β -ME-inhibited *K. aerogenes* urease using EXAFS [45], but it is significantly shorter than that found in native (3.6 Å) [16] or AHA-inhibited C319A (3.7 Å) [19] *K. aerogenes* urease. Considering the rigidity of the coordination bonds of the Ni ions with the protein ligands in urease, such a decrease of the Ni-Ni distance can only be explained by postulating some flexibility of the whole active site, i.e. an ability to adopt slightly different conformations dictated by the intrinsically distinct electronic properties of the bimetallic core in the native (water-bridged Ni dimer) and in the β -ME-bound (thiolate-bridged Ni dimer) forms. In order to confirm this possibility, a structural comparison with synthetic analogue models, for which protein-induced effects are absent, is necessary. A screening of the Cambridge Structural Database reveals that no synthetic μ -thiolato-mono-carboxylato Ni dimers have been structurally characterised. Synthetic Ni dimers featuring a μ -aqua-bis-carboxylato bridge have Ni-Ni distances of 3.48–3.68 Å [51–58], while distances of 3.40

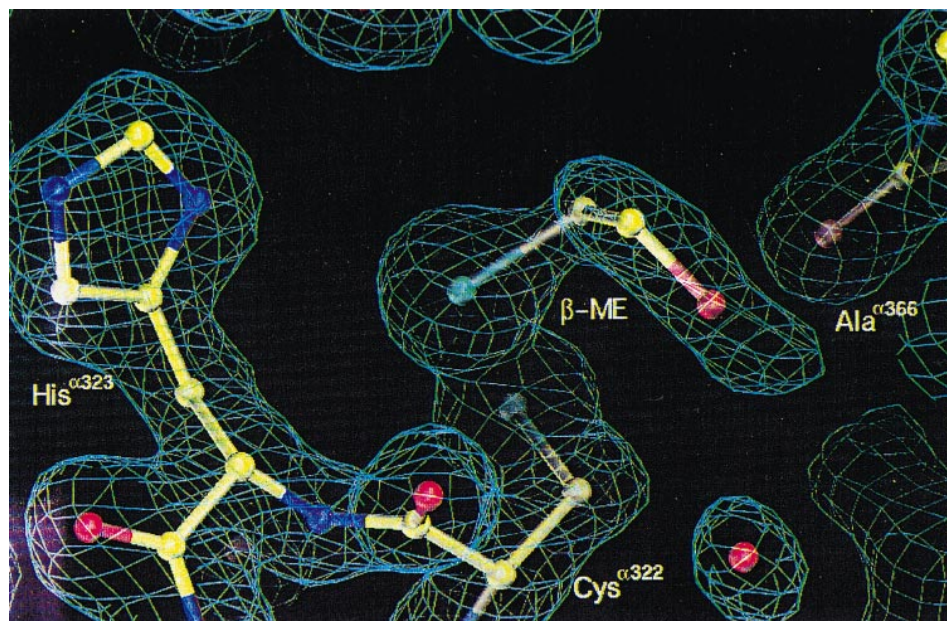


Fig. 4 The atomic model of the active site of β -ME-inhibited *B. pasteurii* urease, showing the second β -ME molecule bound to Cys $^{\alpha 322}$ and hydrogen-bonded to Ala $^{\alpha 366}$, superimposed on the final $2F_0 - F_c$ electron density map contoured at 1σ

\AA and 3.42 \AA are found in μ -hydroxide-bis-carboxylato [59] and μ -phenoxide-bis-carboxylato [60] Ni dimers, respectively. Replacement of one of the carboxylato bridges with an anionic single-atom bridge, as in model compounds featuring either a bis- μ -hydroxamato-mono-acetato [20] or a bis- μ -phenoxide-mono-carboxylato [61] bridged Ni dimer, causes decrease of the Ni-Ni distance to 3.016 and 3.043 \AA , respectively. The Ni-Ni distance found in bis- μ -thiolato dimers is 3.36 \AA in $[\text{Ni}_2(\text{SC}_2\text{H}_5)_6]^{2-}$ [47] or 3.27 \AA in $[\text{Ni}_2(\text{S-}p\text{-C}_6\text{H}_4\text{Cl})_6]^{2-}$ [50], while in $[\text{Ni}_2(\text{ethane-1,2-dithiolate})_3]^{2-}$ it shortens to 2.94 \AA [49] or 2.91 \AA [48], a decrease that has been ascribed to a chelating effect and to the small dihedral angle between the two planes formed by the bridging thiolate sulfur atoms and the two Ni ions in the latter complex [48, 49]. Therefore, in the absence of additional bridging ligands, the short Ni-Ni distance in the μ -thiolato-mono-carboxylato bridged dinickel centre of β -ME-inhibited *B. pasteurii* urease can be considered an intrinsic property of this metallic core, resulting from three additive effects: the presence of an anionic thiolate bridge, the bridging-chelating mode of β -ME, and the small dihedral angle between the equatorial planes of the square- and trigonal-pyramidal coordination spheres of the two Ni ions.

Figure 4 shows that a second molecule of β -ME is involved in a mixed disulfide bond with Cys $^{\alpha 322}$, a residue which is supposed to play a significant role in the catalytic process [62, 63], even though it is not essential [64, 65]. Cys $^{\alpha 322}$ resides on an α -helix that is part of a conserved mobile flap in *K. aerogenes* native urease. This flap has been proposed to act as a gate for the entrance of the substrate to the active site [16, 19] but could also take part in the assembly of the dinickel centre from apo-urease. The β -ME molecule forming the mixed disulfide with Cys $^{\alpha 322}$ in *B. pasteurii*-inhibited

urease is involved in a hydrogen bond between its α -hydroxyl group and the carbonyl oxygen atom of Ala $^{\alpha 366}$, positioned on a neighbouring loop (Figs. 2 and 4). This interaction reduces the flexibility of the flap, and the resulting network seals the entrance to the active site by steric hindrance.

In summary, the X-ray structure of β -ME-inhibited *B. pasteurii* urease reveals that inhibition occurs by targeting enzyme sites that are both directly (the metal centres) and indirectly (the cysteine side chain) participating in substrate positioning and activation. This double inhibition mode is likely to be involved in all cases in which a thiol acts as a urease inhibitor [27, 62]. These structural details, shedding light on the mechanism of inhibition and providing hints for the rational design of new potent urease inhibitors, could not be obtained from the spectroscopic studies so far reported.

To further understand the catalytic and inhibition mechanism of urease, high resolution diffraction data for native *B. pasteurii* urease, as well as for the enzyme inhibited with cysteamine, acetohydroxamic acid, and phenylphosphoradiamidate have recently been collected [28]. Details of these structures and, in particular, the precise location of water, inhibitors, and substrate analogue molecules in the active site of urease, must await the completion of the refinement.

Acknowledgements We thank the European Union for support of the work at EMBL Hamburg through the HCMP Access to Large Installations Project, Contract Number CHGE-CT93-0040. The authors are grateful to Consiglio Nazionale delle Ricerche, Comitato 11 "Tecnologia e Innovazione", for partial funding of the research described in this work, and to EMBL for a predoctoral fellowship to S. B.

References

- Andrews RK, Blakeley RL, Zener B (1989) In: Lancaster JR Jr (ed) Urease – a Ni(II) metalloenzyme. VCH, New York, pp 141–166
- Mobley HLT, Hausinger RP (1989) *Microbiol Rev* 53:85–108
- Hausinger RP (1993) *Biochemistry of nickel*. Plenum, New York
- Mobley HLT, Island MD, Hausinger RP (1995) *Microbiol. Rev* 59:451–480
- Collins CM, D’Orazio SEF (1993) *Mol Microbiol* 9:907–913
- Bremner JM, Krogmeier MJ (1989) *Proc Natl Acad Sci USA* 86:8185–8188
- Bremner JM (1995) *Fert Res* 42:321–329
- Rosenstein IJM, Hamilton-Miller JMT (1984) *Crit Rev Microbiol* 11:1–12
- Bremner JM, Krogmeier MJ (1988) *Proc Natl Acad Sci, USA* 85:4601–4604
- McCarthy GW, Bremner JM, Lee JS (1990) *Plant Soil* 127:269–283
- Griffith DP (1978) *Kidney Int* 13:372–382
- Sim E, Jones A, Stanley L (1985) *Acta Pharmacol Toxicol* 57:304–306
- Krogmeier MJ, McCarty GW, Bremner JM (1989) *Proc Natl Acad Sci, USA* 86:1110–1112
- Hamilton-Miller JMT, Gargan RA (1979) *Invest Urol* 16:327–328
- Jabri E, Carr MB, Hausinger RP, Karplus PA (1995) *Science* 268:998–1004
- Karplus PA, Pearson MA, Hausinger RP (1997) *Acc Chem Res* 30:330–337
- Jabri E, Karplus PA (1996) *Biochemistry* 35:10616–10626
- Park I-S, Michel LO, Pearson MA, Jabri E, Karplus PA, Wang S, Dong J, Scott RA, Koehler BP, Johnson MK, Hausinger RP (1996) *J Biol Chem* 271:18632–18637
- Pearson MA, Overbye Michel L, Hausinger RP, Karplus PA (1997) *Biochemistry* 36:8164–8172
- Stemmler AJ, Kampf JW, Kirk ML, Pecoraro VL (1995) *J Am Chem Soc* 117:6368–6369
- Mulrooney SB, Hausinger RP (1990) *J Bacteriol* 172:5837–5843
- Larson AD, Kallio RE (1954) *J Bacteriol* 68:67–73
- Christians S, Kaltwasser H (1986) *Arch Microbiol* 145:51–55
- Benini S, Gessa C, Ciurli S (1996) *Soil Biol Biochem* 28:819–821
- Moersdorf G, Weinmann P, Kaltwasser H (1994) GenBank accession number X78411
- Benini S, Ciurli S, Nolting HF, Mangani S (1996) *Eur J Biochem* 239:61–66
- Todd MJ, Hausinger RP (1989) *J Biol Chem* 264:15835–15842
- Benini S, Ciurli S, Rypniewski W, Wilson KS, Mangani S (1998) *Acta Crystallogr, D54* (in press)
- van Silfhout RG, Hermes C (1995) *Rev Sci Instr* 66:1818–1820
- Otwinowski Z (1988) DENZO. A program for automatic film evaluation of film intensities. Yale University, New Haven, Conn
- Matthews BW (1968) *J Mol Biol* 33:491–497
- Navaza J (1994) *Acta Crystallogr, A50*:157–163
- Jones TA, Zou JY, Cowan SW, Kjeldgaard M (1991) *Acta Crystallogr, A47*:110–119
- Konnert JH (1976) *Acta Crystallogr A32*:614–617
- Konnert JH, Hendrickson WA (1980) *Acta Crystallogr A36*:344–350
- Murshudov GN, Vagin AA, Dodson EJ (1997) *Acta Cryst D53*:240–255
- Engh RA, Huber R (1991) *Acta Crystallogr A47*:392–400
- Lamzin VS, Wilson KS (1997) *Methods Enzymol* 277:269–305
- Park I-S, Hausinger RP (1993) *Protein Sci* 2:1034–1041
- Blakeley RL, Dixon NE, Zerner B (1983) *Biochim Biophys Acta* 744:219–229
- Nagarajam K, Fishbein WN (1977) *Fed Proc Fed Am Soc Exp Biol* 36:700
- Finnegan MG, Kowal AT, Werth MT, Clark PA, Wilcox DE, Johnson MK (1991) *J Am Chem Soc* 113:4030–4032
- Clark PA, Wilcox DE (1989) *Inorg Chem* 28:1326–1333
- Clark PA, Wilcox DE, Scott RA (1990) *Inorg Chem* 29:579–581
- Wang S, Lee MH, Hausinger RP, Clark PA, Wilcox DE, Scott RA (1994) *Inorg Chem* 33:1589–1593
- Volbeda A, Garcin E, Piras C, Lacey AL de, Fernandez VM, Hatchikian EC, Fray M, Fontecilla-Camps JC (1996) *J Am Chem Soc* 118:12899–12906
- Watson AD, Pulla Rao C, Dorfman R, Holm RH (1985) *Inorg Chem* 24:2820–2826
- Snyder BS, Pulla Rao C, Holm RH (1986) *Aust J Chem* 39:963–974
- Nicholson JR, Christou G, Huffman JC, Folting K (1987) *Polyhedron* 6:863–870
- Colpas GJ, Kumar M, Day RO, Maroney MJ (1990) *Inorg Chem* 29:4779–4788
- Turpeinen U (1976) *Finn Chem Lett* 173–178
- Turpeinen U (1977) *Finn Chem Lett* 36–41
- Turpeinen U, Ahlgren M, Hamalainen R (1977) *Finn Chem Lett* 246–251
- Turpeinen U (1977) *Finn Chem Lett* 123–128
- Ahlgren M, Hamalainen R, Turpeinen U (1977) *Cryst Struct Commun* 6:829–834
- Ahlgren M, Turpeinen U, Hamalainen R (1978) *Acta Chem Scand A32*:189–194
- Ahlgren M, Turpeinen U (1982) *Acta Cryst B38*:276–279
- Wages HE, Taft KL, Lippard SJ (1993) *Inorg Chem* 32:4985–4987
- Chaudhuri P, Kuppers H-J, Wieghardt K, Gehring S, Haase W, Nuber B, Weiss J (1988) *J Chem Soc Dalton Trans* 1367–1370
- Buchanan RM, Mashuta MS, Oberhausen KJ, Richardson JF, Li Q, Hendrickson DN (1989) *J Am Chem Soc* 111:4497–4498
- Nanda KK, Das R, Thompson LK, Venkatsubramanian K, Nag K (1994) *Inorg Chem* 33:5934–5939
- Todd MJ, Hausinger RP (1991) *J Biol Chem* 266:10260–10267
- Todd MJ, Hausinger RP (1991) *J Biol Chem* 266:24327–24331
- Martin PR, Hausinger RP (1992) *J Biol Chem* 267:20024–20027
- Jose J, Schafes K, Kaltwasser H (1994) *Arch Microbiol* 161:384–392